

# Effect of total ionizing dose radiation on the 0.25 $\mu\text{m}$ RF PDSOI nMOSFETs with thin gate oxide\*

Liu Mengxin(刘梦新), Han Zhengsheng(韩郑生)<sup>†</sup>, Bi Jinshun(毕津顺), Fan Xuemei(范雪梅),  
Liu Gang(刘刚), and Du Huan(杜寰)

(Institute of Microelectronics, Chinese Academy of Sciences, Beijing 100029, China)

**Abstract:** Thin gate oxide radio frequency (RF) PDSOI nMOSFETs that are suitable for integration with 0.1  $\mu\text{m}$  SOI CMOS technology are fabricated, and the total ionizing dose radiation responses of the nMOSFETs having four different device structures are characterized and compared for an equivalent gamma dose up to 1 Mrad (Si), using the front and back gate threshold voltages, off-state leakage, transconductance and output characteristics to assess direct current (DC) performance. Moreover, the frequency response of these devices under total ionizing dose radiation is presented, such as small-signal current gain and maximum available/stable gain. The results indicate that all the RF PDSOI nMOSFETs show significant degradation in both DC and RF characteristics after radiation, in particular to the float body nMOS. By comparison with the gate backside body contact (GBBC) structure and the body tied to source (BTS) contact structure, the low barrier body contact (LBBC) structure is more effective and excellent in the hardness of total ionizing dose radiation although there are some sacrifices in drive current, switching speed and high frequency response.

**Key words:** PDSOI; total ionizing dose radiation; RF

**DOI:** 10.1088/1674-4926/30/1/014004

**EEACC:** 1350; 2530F; 2550R

## 1. Introduction

Silicon-on-insulator (SOI) CMOS technology has been a promising candidate for highly integrated, high-performance<sup>[1]</sup> and radio frequency (RF) applications with low power consumption due to its lower parasitic capacitance and substrate RF power loss, higher transconductance, smaller short-channel effects, reduced substrate coupling, elimination of cross-talk and latch-up, process compatibility and full dielectric isolation for high- $Q$  passive components<sup>[2-6]</sup>. Furthermore, properly designed SOI circuits are less susceptible to single event upset (SEU) from energetic particles and can function without upset or failure after exposure to extremely high dose rate pulses of ionizing irradiation as compared to traditional bulk silicon circuits<sup>[7,8]</sup>. However, the total ionizing dose response of SOI ICs is more complex and difficult to harden than bulk silicon ICs due to its thick buried oxide (BOX). The total ionizing dose-related charge trapping and interface trap generation in the BOX layer can induce leakage channels or alter the threshold voltage of SOI MOSFETs<sup>[9,10]</sup>. In addition, the floating body effects inherent in the PDSOI MOSFETs cause unwanted effects such as kinks, anomalous subthreshold current, transient current overshoot and early device breakdown. Therefore, research on the total ionizing dose effects and floating body effects of RF SOI devices has received significant attention in recent years<sup>[11-14]</sup>.

This paper begins with a short description of the major processing steps and the experimental methods of the thin

gate oxide RF PDSOI nMOSFETs, and goes on to evaluate and compare the total ionizing dose radiation response of the nMOSFETs with different device structures for an equivalent gamma dose up to 1 Mrad (Si) at room temperature. Results of the direct current (DC) testing and small-signal RF testing before and after the irradiation are provided and discussed in detail. Then a final conclusion is drawn from the entire work.

## 2. Experiment

The thin gate oxide RF PDSOI nMOSFETs were fabricated on SIMOX (separation by implantation of oxygen) wafers with an SOI film (p-type  $<100>$ , 20  $\Omega$ ) thickness of 200 nm and a buried oxide layer of 400 nm. A summary of the major processing steps of the technology, which are based on the platform of 0.1  $\mu\text{m}$  CMOS technology developed by the Institute of Microelectronics of Chinese Academy of Sciences<sup>[15]</sup>, is given as follows. Prior to the device fabrication, a LOCOS (local oxidation of silicon) approach was employed to isolate the MOSFETs; after that, maskless  $\text{BF}_2^+$  ion implants with energy 80 keV and dose  $2 \times 10^{12} \text{ cm}^{-2}$  and  $\text{B}^+$  ion implants with energy 70 keV and dose  $4 \times 10^{13} \text{ cm}^{-2}$  were employed for front gate threshold voltage adjustment and anti-punch through purpose, respectively. A preferable 6 nm thin gate oxide was grown, followed by deposition of 300 nm polysilicon and  $\text{As}^+$  ion implants with energy 100 keV and dose  $4 \times 10^{15} \text{ cm}^{-2}$  for polysilicon doping; then, an e-beam direct-writing technique was adopted to get a gate length of small dimension. After the

\* Project supported by the National Natural Science Foundation of China (No. 60576051) and the State Key Development Program for Basic Research of China (No. 2006CB3027-01).

<sup>†</sup> Corresponding author. Email: zshan@ime.ac.cn

Received 24 July 2008, received manuscript received 1 September 2008

© 2009 Chinese Institute of Electronics

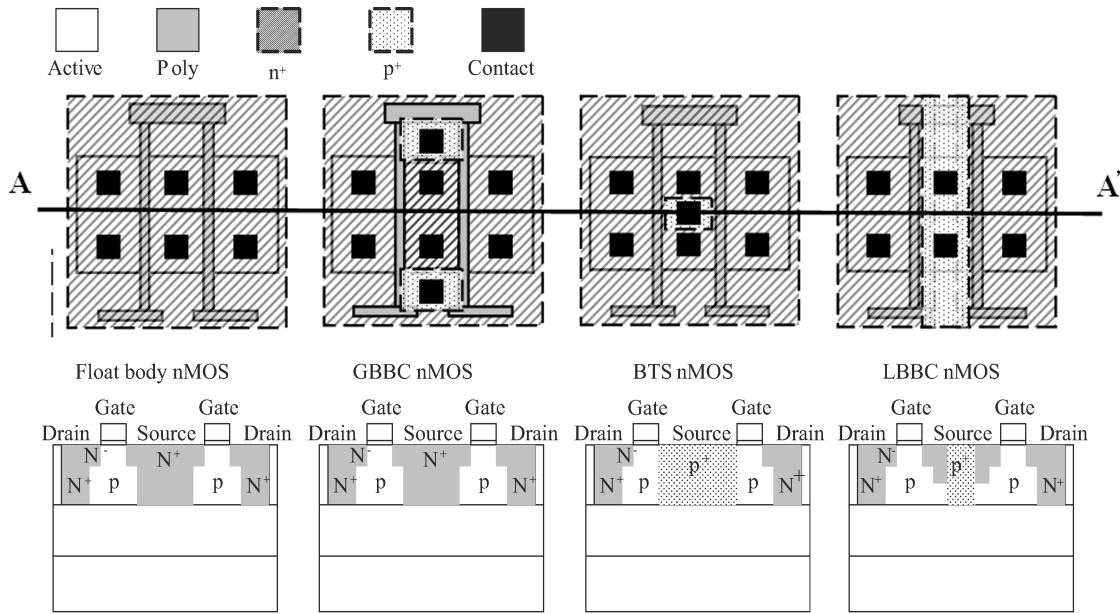


Fig.1. Layouts and cross-sections along line A-A' of the thin gate oxide RF PDSOI nMOSFETs.

gate definition, B<sup>+</sup> ions with energy 25 keV and dose  $1 \times 10^{14} \text{ cm}^{-2}$  were implanted into the source side to form a p<sup>+</sup> layer for body contacts, with the drain masked by photoresist. Then, As<sup>+</sup> LDD implantation with energy 25 keV and dose  $3 \times 10^{14} \text{ cm}^{-2}$  was performed with the body contact region masked by photoresist. After that, tetraethoxysilane (TEOS) oxide was deposited and patterned with the same mask to form the spacer sidewall and the mask oxide on the body contact region, followed by As<sup>+</sup> deep source and drain implantation with energy 25 keV and dose  $5 \times 10^{15} \text{ cm}^{-2}$  and a rapid thermal annealing (RTA) step with 1030 °C annealing for 6 s. The device processes were completed when TiSi<sub>2</sub> salicide was formed on the front/back gate, source and drain regions, and also on the body contact regions, followed by dual layer metallization and passivation.

So far, a thin gate oxide RF PDSOI nMOSFET has taken shape, featuring TiSi<sub>2</sub> salicide and a body contact utilizing the p<sup>+</sup> region. In addition, the nMOSFETs with three different body contact structures, i.e. gate backside body contact (GBBC) structure, low barrier body contact (LBBC) structure and body tied to source (BTS) structure, are compared with the float body nMOSFETs for the purpose of evaluating the validities of these body contacts for total ionizing dose radiation hardening. The schematic layouts and cross-sections along line A-A' of these nMOSFETs are illustrated in Fig.1.

The total ionizing dose radiation response of the individual thin gate oxide RF PDSOI nMOSFETs was characterized using the Co-60 gamma ray irradiation facility at the Chemistry College of Beijing Normal University with a dose rate of 203 rad(Si)/s. The ambient temperature of the testing was 25 °C and the RF PDSOI nMOSFETs chips were mounted on plastic holders and exposed to gamma ray radiation up to 1 Mrad(Si). Immediately after irradiation, on-wafer DC characteristics were measured using a Keithley 4200 Semiconductor Characterization System and small-signal scattering parameters (S-parameters) of the tested devices were ex-

tracted by an Agilent 8510C Vector Network Analyzer connected to a Cascade Microtech Summit 9000 probe station with ground-signal-ground (GSG) pattern probes. The specially designed “open-short” dummy structures were employed to de-embed pad parasitics for the extraction of the small-signal equivalent circuits. In order to exactly reveal the actual radiation RF response of the intrinsic devices after irradiation without the influences of parasitical effects introduced by the package and pad structures, a terminal floating and unpackaged conditions were adopted.

### 3. Results and discussion

#### 3.1. DC performance

The drain current ( $I_{DS}$ ) as a function of front gate voltage ( $V_{FG}$ ) for RF PDSOI nMOSFETs with dimensions of  $W/L = 20 \mu\text{m}/0.25 \mu\text{m}$  at low ( $V_{DS} = 0.1 \text{ V}$ ) and high ( $V_{DS} = 3 \text{ V}$ ) drain voltage, are shown in Fig.2 before and after radiation respectively. The impacts of the three different body contact structures and front gate threshold voltage shifts are also demonstrated in the figure. As shown in Fig.2, the sub-threshold swing ( $S$ ) and front gate threshold voltage ( $V_{FT}$ ) of the nMOS devices increase significantly after 1 Mrad(Si) radiation. Furthermore, a continuous increase of  $V_{FT}$  is observed when the nMOSFETs are subjected to a 290 min anneal at room temperature. This may be mainly attributed to the buildup of the radiation-induced interface traps and border traps at the Si/SiO<sub>2</sub> interface.

The elements most sensitive to ionizing radiation in MOSFETs are the gate and isolation oxides. When the nMOSFETs are exposed to the gamma ray ionizing irradiation, a large number of electron-hole pairs is generated throughout the oxide due to Compton scattering. Immediately after the creation of electron-hole pairs, a fraction of them recombine and the remaining electrons rapidly sweep out of the silicon dioxide owing to their high mobility ( $\sim 20 \text{ cm}^2/(\text{V}\cdot\text{s})$ ) in SiO<sub>2</sub>.

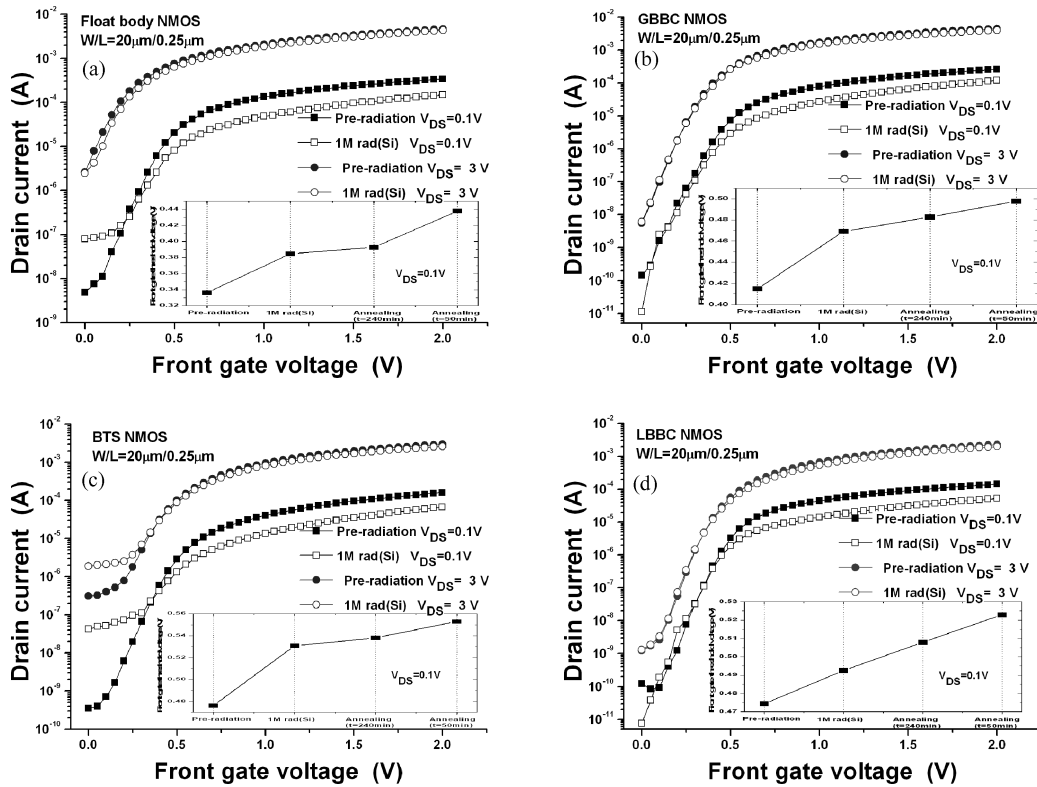


Fig.2. Drain current as a function of front gate voltage for RF PDSOI nMOSFETs with four different structures before and after gamma radiation.

Then the holes that escape the initial recombination will transport through the oxide toward the Si/SiO<sub>2</sub> interface by hopping through polaron states in the oxide, and some fractions of these holes can be trapped by the oxygen vacancies close to the interface, which result from the out-diffusion of oxygen from the oxide and the lattice mismatch between SiO<sub>2</sub> and silicon during device fabrication. Most of these hole oxide traps are predominantly positive. Several seconds after irradiation, a large number of interface traps and border traps begin to build up due to the hole trapping and the dangling bonds between the silicon and the SiO<sub>2</sub>. Considering our thin gate oxide ( $t_{ox} = 6$  nm), the radiation-induced oxide hole trap charge can be easily neutralized by the tunneling of electrons from either the gate or the Si/SiO<sub>2</sub> interface and by the thermal emission of electrons from the oxide valance band. Therefore, the majority of traps in thin oxide may function electrically like interface traps, which are predominantly negatively charged for an n-channel transistor. This will result in positive increases in  $S$  and  $V_{FT}$ . Since the interface traps can hardly be annealed below 125 °C,  $V_{FT}$  will continue to increase during annealing process, which is also presented in Fig.2.

In addition, another important phenomenon observed in Fig.2 is a considerable increase of off-state leakage current ( $I_{leak-off}$ ) of the float body and BTS nMOSFETs. The off-state leakage currents of the float body and BTS nMOS significantly increase from about 5 nA and 350 pA before radiation to about 80 and 40 nA after a total dose of 1 Mrad (Si) at low drain voltage bias, respectively. However, an almost constant or even smaller  $I_{leak-off}$  (below 100 pA) of GBBC and LBBC nMOS is

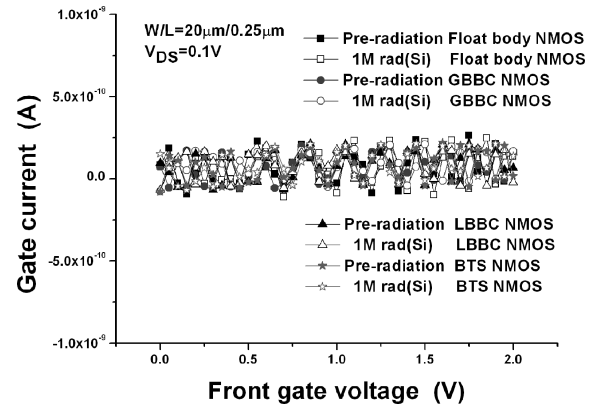


Fig.3. Front gate current as a function of front gate voltage before and after gamma radiation.

observed after irradiation. This difference is attributed to the validities of such body contacts for total ionizing dose radiation hardening.

The primary causes for  $I_{leak-off}$  are front gate leakage, LOCOS field oxide leakage and buried oxide leakage. Figure 3 illustrates the front gate current as a function of front gate voltage for RF PDSOI nMOSFETs with the drain voltage biased at 0.1 V. For radiation exposure up to 1 Mrad (Si), the gate leakage currents barely change (by less than 100 pA) for all the four nMOSFETs. The results indicate that the gate leakage current can be negligible as for total leakage currents of the device. Moreover, the field oxide leakage current is another chief component of the radiation-induced leakage current (RILC). Most radiation-induced oxide traps in LOCOS oxides overlying a p-type surface are predominantly positive. The combination of the gate polysilicon, the oxide in the bird's

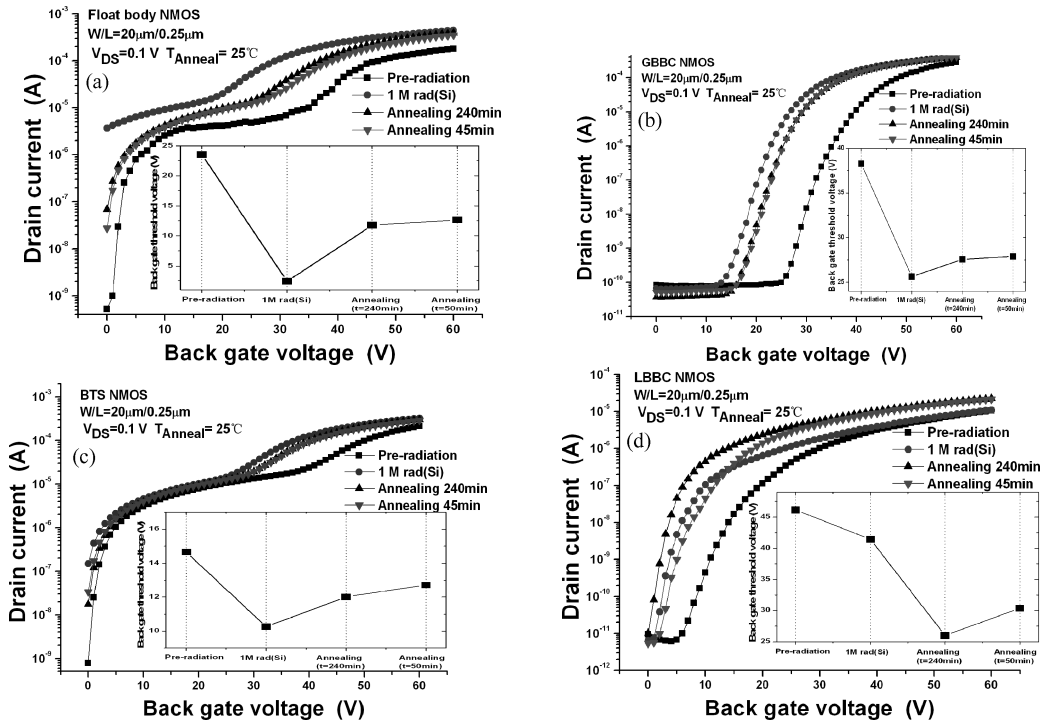


Fig.4. Drain current as a function of back gate voltage for RF PDSOI nMOSFETs with four different body contact structures before and after gamma radiation.

beak of LOCOS and the source and drain form a parasitic edge transistor, which is parallel to the front gate-oxide transistor. The quality of the bird's beak oxide near the LOCOS/front gate oxide interface is likely to be poorer than that of the field isolated oxide, therefore it will be more efficient in trapping charge. The accumulated radiation-induced oxide traps result in a negative shift in the threshold voltage large enough that the parasitic edge transistor triggers off and then produces a conduction path in the off state, thus the leakage current greatly increases. Since the GBBC and LBBC contact structures increase the doping level ( $P^+$ ) in the edge of LOCOS which is the base of the parasitic edge transistor, the amplifying ability of the parasitic edge transistor will be weakened, hence the LOCOS leakage is inhibited.

Charge trapping not only generates a lateral parasitic transistor effect but also a back gate transistor effect. Figure 4 shows the drain current versus back gate voltage ( $V_{BG}$ ) characteristics while the front gate voltage is grounded and the drain voltage biased at 0.1 V. Due to the adoption of low substrate doping concentration, the back gate performances of nMOSFETs are exceedingly sensitive to radiation. As seen in Fig.4, almost all the devices present large negative back gate threshold voltage ( $V_{BT}$ ) shifts after 1 Mrad(Si) radiation and then slowly increase with the annealing time. If the  $V_{BT}$  decreases so much that the back gate transistor becomes conductive without back gate bias (0 V), it can induce a current leakage on the front transistor. Furthermore, the buildup of interface states after exposure to radiation occurs on a much slower time scale than the buildup of oxide-trapped charge. That is why the  $V_{BT}$  declines first and then recovers, as illustrated in Fig.4. Owing to the adoption of  $p^+$  implant near the source for LBBC and GBBC nMOSFETs which is used to form a contact, the  $V_{BT}$

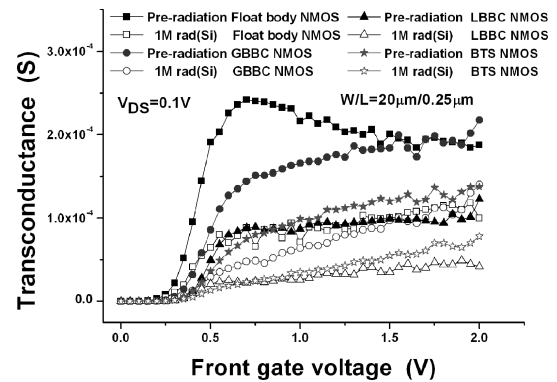


Fig.5. Transconductance as a function of front gate voltage before and after radiation.

of LBBC and GBBC nMOS are nearly double the  $V_{BT}$  of the float body and BTS nMOS. The  $p^+$  implant prevents the inversion of the buried oxide at that location by adjusting the local threshold voltage to a very high value. This suggests that the back parasitic transistor of LBBC and GBBC nMOSFETs is harder to turn on by total ionizing dose radiation, and larger radiation-induced back gate threshold voltage shifts will be tolerated. Consequently the LBBC and GBBC contact structures can show a better total ionizing dose radiation hardness.

Figure 5 shows transconductance ( $g_m$ ) versus front gate voltage at low drain voltage ( $V_{DS}=0.1$  V). Figure 6 shows the output characteristics of RF SOI nMOSFETs before and after 1 Mrad (Si) radiation. Generally,  $g_m$  varies directly with carrier mobility ( $\mu_n$ ) and varies inversely with  $V_{FT}$ , however the drain saturation current is directly proportional to carrier mobility and is inversely proportional to  $V_{FT}^2$ . As for our thin gate oxide RF PDSOI nMOSFETs, the large concentration of radiation-induced interface-trapped charges in the front gate

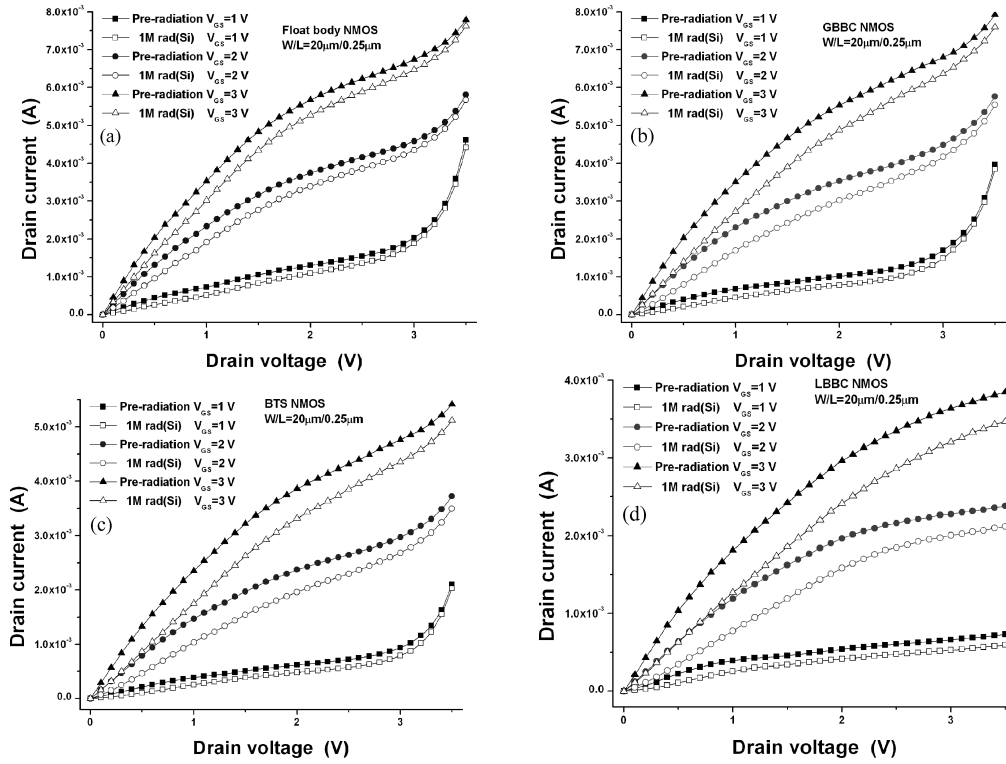


Fig.6. Output characteristics of RF PDSOI NMOSFETs with (a) float body , (b) GBBC contact , (c) BTS contact and (d) LBBC contact before and after gamma radiation.

oxide increases the Coulomb scattering of carriers in the front channel and hence reduces the carrier mobility. Furthermore, the introduction of interface-trapped charges can increase  $V_{FT}$  considerably as mentioned before. As a consequence, both  $I_{Dsat}$  and  $g_m$  degraded noticeably for all the four devices after irradiation with 1 Mrad(Si), which will result in smaller driving ability and slower switching speed respectively. Besides, several significant kink regions are observed in the output characteristics of float body nMOS, GBBC nMOS and BTS nMOS, whereas the LBBC nMOS shows a smooth drain saturation current curve. This reveals that the LBBC contact structure can successfully limit the floating body effect and the amplification of the parasitic bipolar transistor inherent in the PDSOI MOSFETs. But these improvements are acquired by sacrificing the drive current and switching speed of on-state devices. As seen in Fig.6, the magnitude of  $I_{Dsat}$  and  $g_m$  of LBBC nMOS is only half that of the float body nMOS, and the GBBC nMOS and is approximately the same as the BTS nMOS.

As discussed above, in view of the thin gate oxide RF PDSOI nMOSFETs, the total ionizing dose radiation results in positive shifts of the front gate threshold voltage, increases in subthreshold swing and off-state leakage current and decreases in transconductance and drain saturation current. These parametric changes can give rise to a failure of the device to turn on normally, can increase the additional power consumption and reduce the noise margin, switching speed and driving ability. In comparison with the GBBC contact structure and BTS contact structure, the LBBC contact structure is more effective and excellent in the hardness of total ionizing dose radiation when

the RF PDSOI nMOSFETs operate in quasi-stationary mode.

### 3.2. RF performance

The  $S$ -parameters of the devices were measured from 100 MHz to 20.1 GHz, and the cut-off frequency ( $f_T$ ) and the maximum oscillation frequency ( $f_{max}$ ) were calculated by extrapolating at a slope of  $-20$  dB/decade from small-signal current gain ( $h_{21}$ ) and maximum available/stable gain ( $G_{max}$ ), respectively. Figure 7 illustrates the variations with frequency of the small-signal current gain  $h_{21}$  and power gain  $G_{max}$  before and after 1 Mrad(Si) radiation with the drain voltage biased at 3 V and the front gate voltage biased at 2 V, considering the four different device structures of the thin gate oxide RF PDSOI nMOSFETs with  $W/L = 20 \mu\text{m}/0.25 \mu\text{m}$ . Several evident degradations in  $h_{21}$  and  $G_{max}$ , whether float body nMOS or GBBC nMOS or BTS nMOS or LBBC, are observed after radiation, indicating that both the small-signal current gain and the power gain are relatively vulnerable to total ionizing dose radiation. However, the RF PDSOI nMOSFET with LBBC contact structure has the lowest radiation-induced exacerbation of its high frequency performance among the structures although its  $f_T$  and  $f_{max}$  are not the best. This is clearer in Table 1, in which the  $f_T$  and  $f_{max}$  as a function of front gate bias voltage are summarized after 1 Mrad(Si) radiation with the drain voltage biased at 3 V. For instance, when the front gate voltage is biased at 2 V and the drain voltage at 3 V, the  $f_T$  and  $f_{max}$  of the LBBC nMOS are 7.179 and 6.911 GHz prior to the irradiation, and 4.919 and 6.073 GHz after 1 Mrad(Si) respectively, which degenerate 31.48% and 12.13%. Nevertheless, the  $f_T$  and  $f_{max}$  of the GBBC nMOS degenerate 33.53% and

Table 1. Summary of cutoff frequency ( $f_T$ ) and maximum oscillation frequency ( $f_{max}$ ) of RF PDSOI nMOSFETs before and after gamma radiation.

Frequency (GHz)		$f_T$		$f_{max}$	
		$V_{FG} = 1\text{ V}$			
Pre-radiation	Float body nMOS	18.294	15.256	17.489	12.102
	GBBC nMOS	13.168	11.541	10.858	10.461
	BTS nMOS	10.819	11.099	8.581	7.718
	LBBC BMOS	6.721	7.179	8.264	6.911
1 Mrad (Si)	Float body nMOS	7.597	7.262	7.435	6.453
	GBBC nMOS	8.718	7.671	6.833	6.288
	BTS nMOS	4.531	5.541	5.766	5.583
	LBBC BMOS	4.022	4.919	7.273	6.073

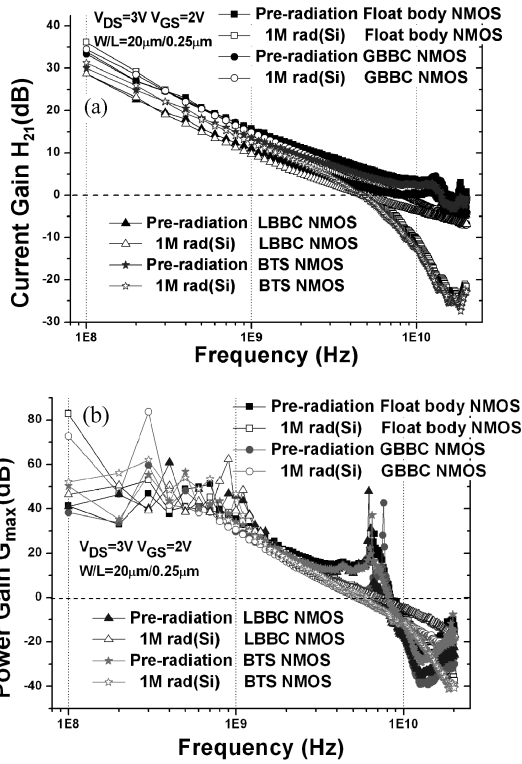


Fig.7. (a) Small-signal current gain and (b) maximum available/stable gain of RF PDSOI nMOSFETs before and after gamma radiation.

39.63%, the  $f_T$  and  $f_{max}$  of the BTS nMOS degenerate 50.08% and 27.66%, and the  $f_T$  and  $f_{max}$  of the float body nMOS degenerate 52.34% and 46.68%, which is the biggest deterioration.

Generally,  $f_T$  and  $f_{max}$  can be given by<sup>[16]</sup>:

$$f_T = \frac{g_m}{2\pi \sqrt{C_g^2 - (g_m R_g + i C_{gs} - C_{gs})^2}} \approx \frac{g_m}{2\pi C_g} \Big|_{C_g=C_{gs}+C_{gd}} \quad (1)$$

$$f_{max} = \frac{f_T}{2 \sqrt{g_{ds} (R_g + R_s) + 2\pi f_T R_g C_{gd}}} \approx \frac{g_m^2 R_L}{2\pi C_g} \Big|_{C_g=C_{gs}+C_{gd}} \quad (2)$$

As shown in Table 1, almost all the RF PDSOI nMOSFETs present a significant degradation in  $f_T$  and  $f_{max}$  after irradiation,

which is mainly due to the decrease of  $g_m$  and  $\mu_n$  as has been explained in section 3.1. All this research and observation enables us to conclude that the LBBC body contact structure is advantageous in total ionizing dose radiation hardness as compared with the BTS and GBBC body contact structures when the thin gate oxide RF PDSOI nMOSFETs operate in alternating current mode.

#### 4. Conclusion

In conclusion, thin gate oxide RF PDSOI nMOSFETs which are suitable for integration with 0.1  $\mu\text{m}$  SOI CMOS technology have been fabricated. The total ionizing dose radiation response of the nMOSFETs having four different device structures was characterized and compared for an equivalent gamma dose up to 1 Mrad (Si), using the front and back gate threshold voltages, off-state leakage, transconductance and output characteristics to assess DC performance. Moreover, the frequency response of these devices under total ionizing dose radiation is presented, such as small-signal current gain and maximum available/stable gain. From the experimental results, it can clearly be seen that all the RF PDSOI nMOSFETs show obvious degradations in both DC and RF characteristics after radiation, in particular for the float body nMOS. By comparison with the GBBC contact structure and the BTS contact structure, the LBBC contact structure is more effective and excellent in the hardness of total ionizing dose radiation although it sacrifices the drive current, switching speed and high frequency response. Therefore, these non-hardened RF PDSOI devices should be optimized in our next work to make them well-suited for applications in an ionizing radiation environment.

#### Acknowledgment

The authors would like to thank Dr. Yang Rong of the Semiconductor Process Technologies Laboratory of Institute of Microelectronics, Singapore, for his previous work and valuable advice.

#### References

[1] Kuo J B, Lin S C. Low-voltage SOI CMOS VLSI devices and

- circuits. New York: John Wiley & Sons Inc, 2001
- [2] Huang R, Liao H, Zhang G. SOI CMOS technology for RF/MMIC applications—yes or no. Proc ESSDRERC, 2005: 241
- [3] Li Junfeng, Yang Rong, Zhao Yuyin, et al. 0.25  $\mu\text{m}$  SOI RF nMOSFETs depleted partially. Chinese Journal of Semiconductors, 2004, 25(9): 1061
- [4] Yang Rong, Qian He, Li Junfeng, et al. SOI technology for radio-frequency integrated-circuit applications. IEEE Trans Electron Devices, 2006, 53(6): 1310
- [5] Eggert D, Huebler P, Huerrich A, et al. A SOI-RF-CMOS technology on high resistivity SIMOX substrates for microwave applications to 5 GHz. IEEE Trans Electron Devices, 1997, 44(11): 1981
- [6] Bi Jinshun, Hai Chaohe. Off-state breakdown characteristics of PDSOI nMOSFETs. Chinese Journal of Semiconductors, 2007, 28(1): 14
- [7] Ma T P, Dressendorfer P V. Ionizing radiation effects in MOS devices and circuits. New York: Wiley & Sons Inc, 1989
- [8] Chen Panxun. Radiation effects on semiconductor devices and integrated circuits. Beijing: National Defense Industry Press, 2005 (in Chinese)
- [9] Schwank J R, Ferlet-Cavrois V, Shaneyfelt M R, et al. Radiation effects in SOI technologies. IEEE Trans Nucl Sci, 2003, 50(3): 522
- [10] Barnaby H J. Total-ionizing-dose effects in modern CMOS technologies. IEEE Trans Nucl Sci, 2006, 53(6): 3103
- [11] Zhao Kai, Liu Zhongli, Yu Fang, et al. Radiation-hardened 128 kb PDSOI CMOS static RAM. Chinese Journal of Semiconductors, 2007, 28(7): 1139 (in Chinese)
- [12] Venkataraman S, Haugerud B M, Zhao E, et al. Impact of proton irradiation on the RF performance of 0.12  $\mu\text{m}$  CMOS technology. 43rd Annual International Reliability Physics Symposium, 2005: 356
- [13] Li Y, Cressler J D, Lu Y, et al. Proton tolerance of multiple-threshold voltage and multiple-breakdown voltage CMOS device design points in a 0.18  $\mu\text{m}$  system-on-a-chip CMOS technology. IEEE Trans Nucl Sci, 2003, 50(6): 1834
- [14] Chen W, Pouget V, Gentry G K, et al. Radiation hardened by design RF circuits implemented in 0.13  $\mu\text{m}$  CMOS technology. IEEE Trans Nucl Sci, 2006, 53(6): 3449
- [15] Xu Qiuxia, Qian He, Yin Huaxiang, et al. High performance 70 nm CMOS devices. Chinese Journal of Semiconductors, 2001, 22(2): 134
- [16] Baliga B J. Silicon RF power MOSFETS. Singapore: World Scientific Publishing Co Pte Ltd, 2005: 33